Results in Physics 10 (2018) 81–90

Contents lists available at ScienceDirect

Results in Physics

journal homepage: www.elsevier.com/locate/rinp

Estimating and understanding the efficiency of nanoparticles in enhancing the conductivity of carbon nanotube/polymer composites

A. Mora, F. Han, G. Lubineau*

King Abdullah University of Science and Technology (KAUST), Physical Science and Engineering Division, COHMAS Laboratory, Thuwal 23955-6900, Saudi Arabia

ARTICLE INFO

Keywords:
Carbon nanotube
Composites
Electrical conductivity
Representative volume element
Geometric modeling

ABSTRACT

Carbon nanotubes (CNTs) have been widely used to improve the electrical conductivity of polymers. However, not all CNTs actively participate in the conduction of electricity since they have to be close to each other to form a conductive network. The amount of active CNTs is rarely discussed as it is not captured by percolation theory. However, this amount is a very important information that could be used in a definition of loading efficiency for CNTs (and, in general, for any nanofiller). Thus, we develop a computational tool to quantify the amount of CNTs that actively participates in the conductive network. We then use this quantity to propose a definition of loading efficiency. We compare our results with an expression presented in the literature for the fraction of percolated CNTs (although not presented as a definition of efficiency). We found that this expression underestimates the fraction of percolated CNTs. We thus propose an improved estimation. We also study how efficiency changes with CNT loading and the CNT aspect ratio. We use this concept to study the size of the representative volume element (RVE) for polymers loaded with CNTs, which has received little attention in the past. Here, we find the size of RVE based on both loading efficiency and electrical conductivity such that the scales of "morphological" and "functional" RVEs can be compared. Additionally, we study the relations between particle and network properties (such as efficiency, CNT conductivity and junction resistance) and the conductivity of CNT/polymer composites. We present a series of recommendations to improve the conductivity of a composite based on our simulation results.

1. Introduction

Carbon nanotubes (CNTs) are ideal nanofillers either to improve the electrical conductivity of polymers [47,49] or to tailor their piezoresistive behavior, making them suitable as strain sensors and for structural health monitoring applications [1,33,55]. CNT-filled polymers are also useful for applications that are constrained by electrical charge mitigation [41]. Increasing the electrical conductivity of the polymer by the addition of CNTs reduces the polymer's dielectric properties. This, in turn, reduces the accumulation of electrical charge, preventing damage to electronic equipment due to electric discharge [19].

The addition of CNTs to a polymer matrix modifies its electrical properties through a percolation process [43]. An important quantity is the percolation threshold, which describes the minimum concentration that ensures the development of one or multiple percolated network(s) from one side to the other side of the sample. For such conductive networks to form, the conductive nanofillers need to be close to each other because conduction between particles is impossible when the nanofillers are separated by more than a few nanometers [24,44]. Due to this limitation, nanofillers that are not close enough to the network will not be part of it. The amount of CNTs that actively participates in the conduction of electricity is unknown and has been largely ignored in the literature. In this work, we quantify the amount of CNTs that actively participates in the conduction of electricity. We use this quantity to provide a definition of loading efficiency that has not been yet offered in the literature. To achieve this, we develop a computational tool that generates geometric representations of CNT networks. We use this tool to study the loading efficiency of polymers filled with CNTs at different volume fractions and aspect ratios. This tool is based on our previous work and has been shown to reproduce realistic CNT networks [15]. An empirical expression to approximate the fraction of percolated CNTs was proposed by Deng and Zheng [10]. However, this expression was not presented as a definition of loading efficiency nor were its limitations studied. Considering that this expression continues to be used [14,28,52], we highlight the importance of studying the validity and limitations of this expression. Thus, we compare our efficiency results with those obtained by the expression presented by Deng

* Corresponding author.
E-mail address: gilles.lubineau@kaust.edu.sa (G. Lubineau).

https://doi.org/10.1016/j.rinp.2018.05.019
Received 16 April 2018; Accepted 8 May 2018
Available online 22 May 2018

and Zheng [10] and present an improved estimation for the fraction of percolated CNTs.

For simulations and measurements to be reliable, they need to be performed on a sample that is at least the size of the representative volume element (RVE). The RVE is the minimum volume at which a property becomes size-independent. The concept of RVE for CNT/polymer nanocomposites has been rarely investigated in the literature and is commonly defined as the simulated volume [33,51]. In other studies, the RVE has been defined as having enough fillers without providing an exact geometry [12]. Periodic unit cells have been defined as RVEs [39]. However, periodicity is not representative of an actual CNT/polymer composite, especially when percolation has to be accurately described. Song et al. [42] obtained the RVE size for a single CNT geometry and used that same RVE size to perform simulations of CNTs with different geometries. However, they did not investigate the dependence of the RVE size on CNT loading or CNT geometry. Lubineau et al. [27] also obtained the RVE size for CNT/polymer composites and considered its dependency on CNT loading, aspect ratio and tortuosity. Here, we build on the results obtained by Lubineau et al. [27] and use electrical conductivity (providing a "functional" definition) and loading efficiency (providing a "morphological" definition) to better understand how to define the RVE size of CNT/polymer composites.

This paper is organized as follows. In Section 2, we present the methodology to generate computational representations of CNT networks and the procedure to determine the backbone and the electrical conductivity of those networks. In this section, we introduce a definition of loading efficiency based on the backbone of the CNT network. In Section 3, we determine the RVE size based on efficiency and electrical conductivity. We compare our results on efficiency with the fraction of percolated CNTs proposed by Deng and Zheng [10] to propose an improved estimation. Additionally, we perform a sensitivity analysis of our model on the electrical conductivity of CNTs and junction resistance. We present recommendations to improve the efficiency and electrical conductivity of CNT/polymer composites based on these results. Finally, we offer conclusions in Section 4.

2. Numerical modeling for RVE determination

2.1. Geometric representation of a CNT network

The algorithm presented by Lubineau et al. [27] is utilized to generate computational representations of CNT networks in cubic samples of size $[a \times a \times a]$. This algorithm is briefly summarized here. For further details, we refer the reader to the original study [27].

In a global Cartesian coordinate system defined by $(\boldsymbol{x}, \boldsymbol{y}, \boldsymbol{z})$, a CNT comprises n interconnected cylinders with length l and radius r, as shown in Fig. 1. The axis of the $(i + 1)$-th cylinder, for $0 \leqslant i \leqslant n-1$, is a segment from point s_i to point s_{i+1}. The starting point of a CNT, s_0, is generated randomly following a uniform distribution in the cube. A local Cartesian coordinate system $(\boldsymbol{x}_i, \boldsymbol{y}_i, \boldsymbol{z}_i)$ with origin at s_i is defined

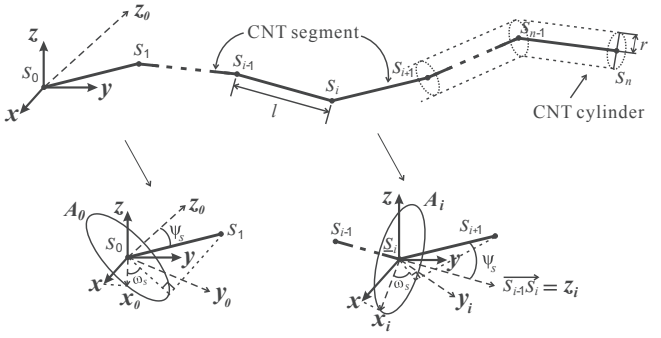

Fig. 1. Geometrical representation of a CNT.

to generate the point s_{i+1} $(0 \leqslant i \leqslant n-1)$. In this local coordinate system, $\boldsymbol{x}_i$ is the projection of $\boldsymbol{x}$ on A_i, where A_i is the plane containing the point s_i with normal vector $\boldsymbol{z}_i$. Here, for $i = 0$, the direction vector $\boldsymbol{z}_0$ is calculated differently from [27]. First, three numbers, v_x, v_y and v_z, are generated randomly following a uniform distribution in the interval $[-1, 1]$. These three numbers define the components of a vector $\boldsymbol{v} = [v_x, v_y, v_z]^T$. Then, we set $\boldsymbol{z}_0 = \boldsymbol{v}/(\boldsymbol{v}\cdot\boldsymbol{v})$. For $1 \leqslant i \leqslant n-1$, $\boldsymbol{z}_i$ has the same direction as $\overrightarrow{s_{i-1}s_i}$. Then, the point s_{i+1} has spherical coordinates (l, ω_s, ψ_s) in the local coordinate system $(\boldsymbol{x}_i, \boldsymbol{y}_i, \boldsymbol{z}_i)$.

Different specifications for the ranges and probability functions for ω_s and ψ_s result in networks with different microstructures such as random or aligned CNTs [15]. Finally, the interpenetration of CNTs during the generation process is avoided to reproduce more realistic CNT networks. Details on how to avoid the interpenetration of CNTs are presented in [27].

2.2. Loading efficiency

Electrical conductivity is possible through a percolated network formed by the CNTs inside the polymer. However, not all CNTs form part of the percolated network nor all CNTs in the percolated network contribute to electrical conductivity. An illustration of this is the 2D network shown in Fig. 2(a). In this network, the CNTs can be separated into an electrically percolated network and some isolated particles, or clusters of particles, that do not participate in the electrical conduction (Fig. 2(b)). The percolated network can be further separated into: 1) the backbone, which is the current carrying member of the percolated network, 2) some zero-current branches that do not bear any current despite their connection to the percolated network, and 3) some balanced branches that form closed loops that do not bear any current either.

Since it is only the backbone network that actually carries electricity, extracting the backbone from a percolated network becomes an important task. In previous work, we described a methodology to extract the backbone from a CNT network [27], which we briefly summarize here.

We start by finding and grouping all CNTs in electrical contact into clusters, by using the Hoshen-Kopelman algorithm [2,17]. We consider two CNTs to be in electrical contact when they are separated by less than the maximum distance that allows transfer of electrons due to tunneling or hopping of electrons [31]. Here, we use a commonly used cutoff distance of $d_t = 1.8$ nm [24].

We then find the percolated clusters, i.e., those clusters that span from one boundary to the opposite one in a cubic sample. The backbone network is extracted from each percolated cluster by applying the direct electrifying algorithm (DEA) [21,22]. This algorithm turns the CNT network into a network of electrical resistors. Then, using the current-carrying definition of the backbone, zero-current paths are found. This network consists of two types of resistors: junction resistors and CNT resistors. When two CNTs are in electrical contact, a junction resistor is added. On the other hand, a CNT resistor comes from the intrinsic electrical resistance of a CNT. Thus, every CNT is initially represented as a resistor. However, when a junction resistor is added between two CNTs, each CNT is divided into two CNT resistors, as shown in Fig. 3.

Next, a voltage is applied to the network of resistors. Then, the system of equations that determines the voltage distribution over the resistor network is solved. Once the voltage at each resistor is known, the current passing through each resistor is calculated. Only those resistors that possess a non-zero current belong to the backbone. For numerical stability and solely to extract the backbone, all resistors are set to 1 Ω. Because of the large differences in magnitude between CNT resistors and junction resistors (e.g., around 1.2×10^5 Ω [27] and 10^{18} Ω [9,24], respectively), having these values in the same matrix causes it to be ill-conditioned. Then, the conditioning number of the matrix is improved by using resistors that have the same magnitude. In addition,

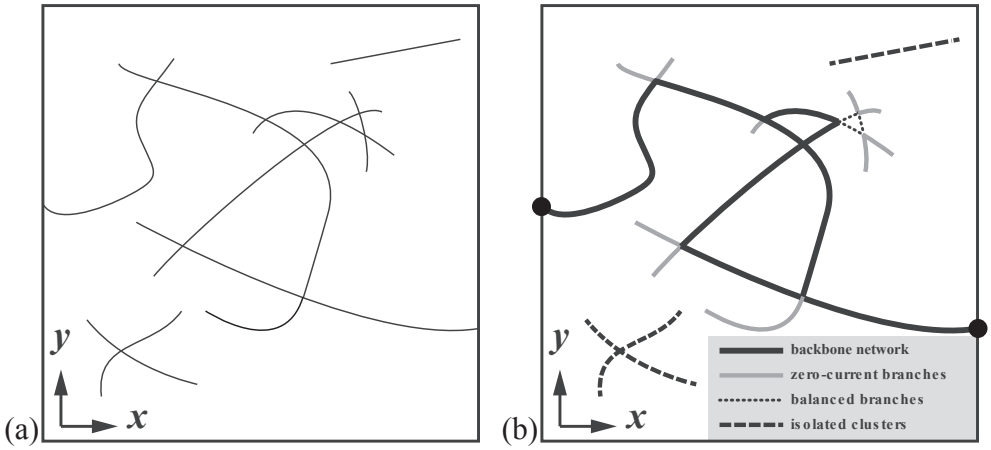

Fig. 2. Example of the classification of CNTs in a simple 2D network.

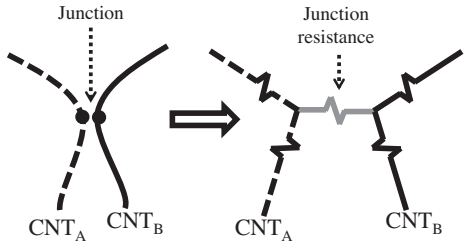

Fig. 3. On the left, two CNTs are shown in electrical contact. The corresponding network of resistors for the direct electrifying algorithm is represented on the right.

the number of iterations to solve the system of equations is reduced. We note that this does not affect our ability to find the backbone because a non-zero current is what defines a resistor as being part of the backbone, not the magnitude of the current.

Finally, as it is clear that the backbone of a CNT network is what actually carries electrical current, we define the loading efficiency, f_{eff}, as the fraction of CNTs that forms part of the backbone:

$$f_{eff} = \frac{V_{backbone}}{V_{tot}} \tag{1}$$

where $V_{backbone}$ is the volume of CNTs that form part of the backbone, and V_{tot}, is the total volume of CNTs inside the sample.

2.3. Electrical conductivity of a CNT network

Here, we consider the electrical conductivity of the nanocomposite (i.e., cubic samples in our model) to be that of the CNT network. We make this assumption because, for loadings larger than the percolation threshold, the CNT network is the main contributor to the composite's conductivity. This is due to the large differences between the electrical conductivities of CNTs and polymers. However, for loadings lower than the percolation threshold, the polymer matrix is the main contributor to the composite's conductivity. For such cases, it is more suitable to obtain the composite's conductivity using a micromechanics approach (e.g., [10,38]).

To estimate the equivalent electrical resistance of the resistor network, R_{eq}, the DEA is applied to its backbone. Estimations of CNT and junction resistors are calculated as follows. The magnitudes of the CNT resistors are obtained using their geometry and CNT conductivity values reported in the literature. The junction resistance is commonly approximated as a function that grows exponentially with respect to the separation between particles [24,18]. However, several factors influence the magnitude of the juncton resistance (e.g., CNT type, CNT diameter, polymer type, junction area [6,13,23]). Thus, it is difficult to obtain an accurate magnitude of the junction resistance. Because of this, the junction resistance has been approximated using a constant value or by obtaining it using a probability distribution function [23–25,40,51]. Since the magnitudes of some CNT resistors are comparable to those of junction resistances [27], we use a constant value for the junction resistance that is higher than that of CNT resistors in the network. This value is calibrated macroscopically as described in the next section.

Next, the current passing through the CNT network is calculated. Finally, using Ohm's law, the value of the equivalent resistance, R_{eq}, of the network is obtained. We can determine the electrical conductivity of the sample, σ, using the following equation:

$$\sigma = \frac{l_{sample}}{R_{eq}A_{sample}} = \frac{1}{aR_{eq}} \tag{2}$$

where $l_{sample} = a$ is the side length of the cubic sample and $A_{sample} = a^2$ is its cross sectional area.

2.4. RVE determination

We base the definition of RVE on the stabilization of a property of interest inside a cubic sample. Here, stabilization means that the property of interest remains constant, or nearly constant, above the size of the RVE and at any point in the material. In this paper, we consider the loading efficiency and the electrical conductivity of the sample as the properties of interest. Thus, we seek to find an RVE based on efficiency and one based on electrical conductivity, resulting in a "morphological" and a "functional" RVE, respectively. To do so, we follow a procedure based on the one described by Lubineau et al. [27], which is briefly summarized here.

We start by defining an observation window of size $[b \times b \times b]$ inside our sample of size $[a \times a \times a]$, where $b < a$. The size of the observation window is progressively increased by increments of Δb. The initial observation window is centered inside the sample and stays centered as the size of the window increases. The size of the observation window is increased until it reaches the size of the sample (i.e., when $a = b$). At each observation window, CNT efficiency and electrical conductivity are calculated. An example illustrating this process is presented in Fig. 4. In this figure, we show the evolution of the electrically conductive backbone for a sample with 0.7 % volume fraction, a=1 μm, 0.5 μm ⩽ b⩽1 μm and Δb = 0.25 μm. The minimum observation window ensuring that CNT efficiency (electrical conductivity) becomes size-independent is considered the efficiency (conductivity)-based RVE.

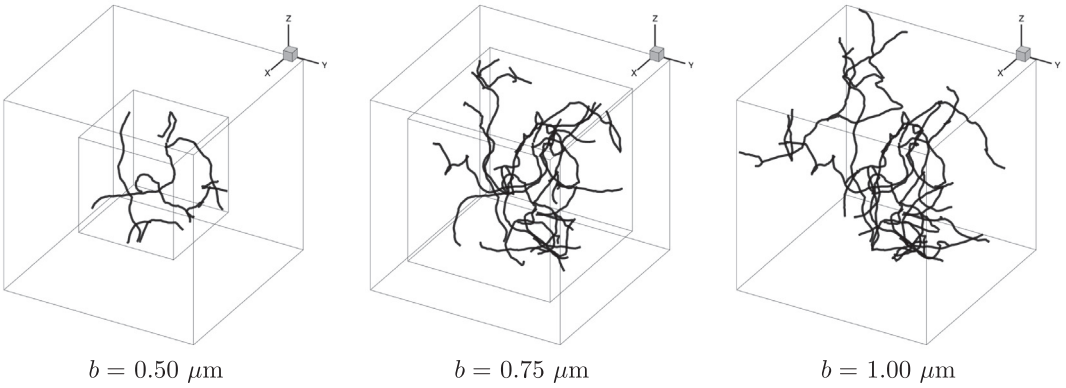

Fig. 4. An example of the process of finding the RVE in a sample with 0.7% volume fraction, a = 1 μm, 0.5 ⩽ *b*⩽ 1 μm and Δb = 0.25 μm. Only the backbone is shown at each observation window.

3. Results and discussion

3.1. Percolation threshold

An important parameter in the study of CNT network conductivity is the percolation threshold, ϕ_c. Here, we run simulations for CNTs of radius 5 nm and lengths 1, 5 and 10 μm. These geometries result in aspect ratios, *AR*, of 100, 500 and 1000, respectively, that are common in experiments [3]. We run simulations to find the percolation threshold for these geometries by proceeding as follows: first, for a given aspect ratio, we determine a suitable range of volume fractions that contains ϕ_c. For instance, for CNTs with *AR*= 100, we find a suitable range to be [0.6%, 0.7%]. We then run simulations for *n* volume fractions inside the given range. After several repetitions, the minimum volume fraction that always results in a percolated network is selected to be the percolation threshold. For instance, for CNTs with *AR* = 100, we set *n* = 401, resulting in a difference of 2.5×10^{-4} between two volume fractions. We consider this accuracy to be sufficient for our simulations. The percolation thresholds found using this method are summarized in Table 1. We note that ϕ_c is reduced as the aspect ratio is increased, as largely reported in the literature [26,31,47] and these results are consistent with those derived from classical analytical models for percolation.

3.2. RVE size determination based on efficiency

We first determine the RVE size based on filler efficiency. The RVE size is determined for each aspect ratio defined in Section 3.1, and at volume fractions ranging from $1.25\phi_c$ to $2.25\phi_c$. In other words, the simulated volume fractions are between 25 % and 125 % above the percolation threshold.

In the left column of Fig. 5, we show the efficiency (as defined by Eq. 1) at each normalized observation window, b/l_{CNT}, where each point is an average over 20 samples. This way, the window size is relative to the length of the CNT. The right column of Fig. 5 shows the relative standard deviation of the efficiency, at each normalized observation window. Each row of Fig. 5 corresponds to a different CNT content, each one given in the form of the reduced volume fraction [4,8,37,49], i.e. as ϕ/ϕ_c-1, where ϕ is the overall volume fraction.

Table 1
Percolation threshold, ϕ_c, for CNT networks with different aspect ratios and CNT lengths.

Aspect ratio	CNT length [μm]	ϕ_c [%]
100	1	0.6325
500	5	0.1387
1000	10	0.07345

In the left column of Fig. 5, when the reduced volume fraction is the same, we observe that the efficiency is similar for all aspect ratios. To the best of our knowledge, this is the first time this conclusion is reported. As the reduced volume fraction is increased, the efficiency also increases for all aspect ratios. We also observe that, as the normalized observation window is increased, the efficiency reaches a plateau, which corresponds to a stabilization of the loading efficiency. We observe that the stabilized efficiency values are actually low for all reduced volume fractions shown in Fig. 5. For example, even at a loading 125 % above the percolation threshold, not even half the CNTs actively participate in the conduction of electricity. These results show that random networks are actually inefficient. These low efficiency values explain the large differences in electrical conductivity compared to segregated structures [35]. In a segregated structure, nanofillers are confined to specific locations in a composite. In this way, nanofillers are more likely to be in contact with each other, thus improving the loading efficiency.

The plots of the relative standard deviation (right column of Fig. 5) show that, at a given reduced volume fraction, there is a rapid decrease of the relative standard deviation as the observation window is increased. This decrease in the relative standard deviation means a reduction of the variability of the loading efficiency. Therefore, the observation window at which this variability is small enough, is chosen as the RVE size. As in our previous work [27], we determine the size of the RVE by defining a threshold equal to 5 % of the maximum relative standard deviation. That is, the observation window at which the relative standard deviation is below this threshold is taken to be the size of RVE. This threshold is represented by a horizontal line in Fig. 5(b), (d), (f), and (h).

3.3. RVE size determination based on electrical conductivity

Here, we determine the size of the RVE based on electrical conductivity for aspect ratios and volume fractions identical to those used in Section 3.2. In previous work, we showed that our simulation results on electrical conductivity agree well with those reported in the literature [30]. Our results here are thus representative of actual composites. Results from our simulations are presented in Fig. 6. The left column of Fig. 6 shows the electrical conductivity along the three directions for all aspect ratios at each normalized observation window, b/l_{CNT}, where each point is an average of 20 samples. The right column of Fig. 6 shows the relative standard deviation of the electrical conductivity at each normalized observation window. Each row of Fig. 6 corresponds to a different reduced volume fraction.

The left column of Fig. 6 clearly shows that the electrical conductivity is anisotropic when the observation window, CNT loading, and aspect ratio are all small. When any of these parameters is increased, and the other two are kept constant, the anisotropy of the

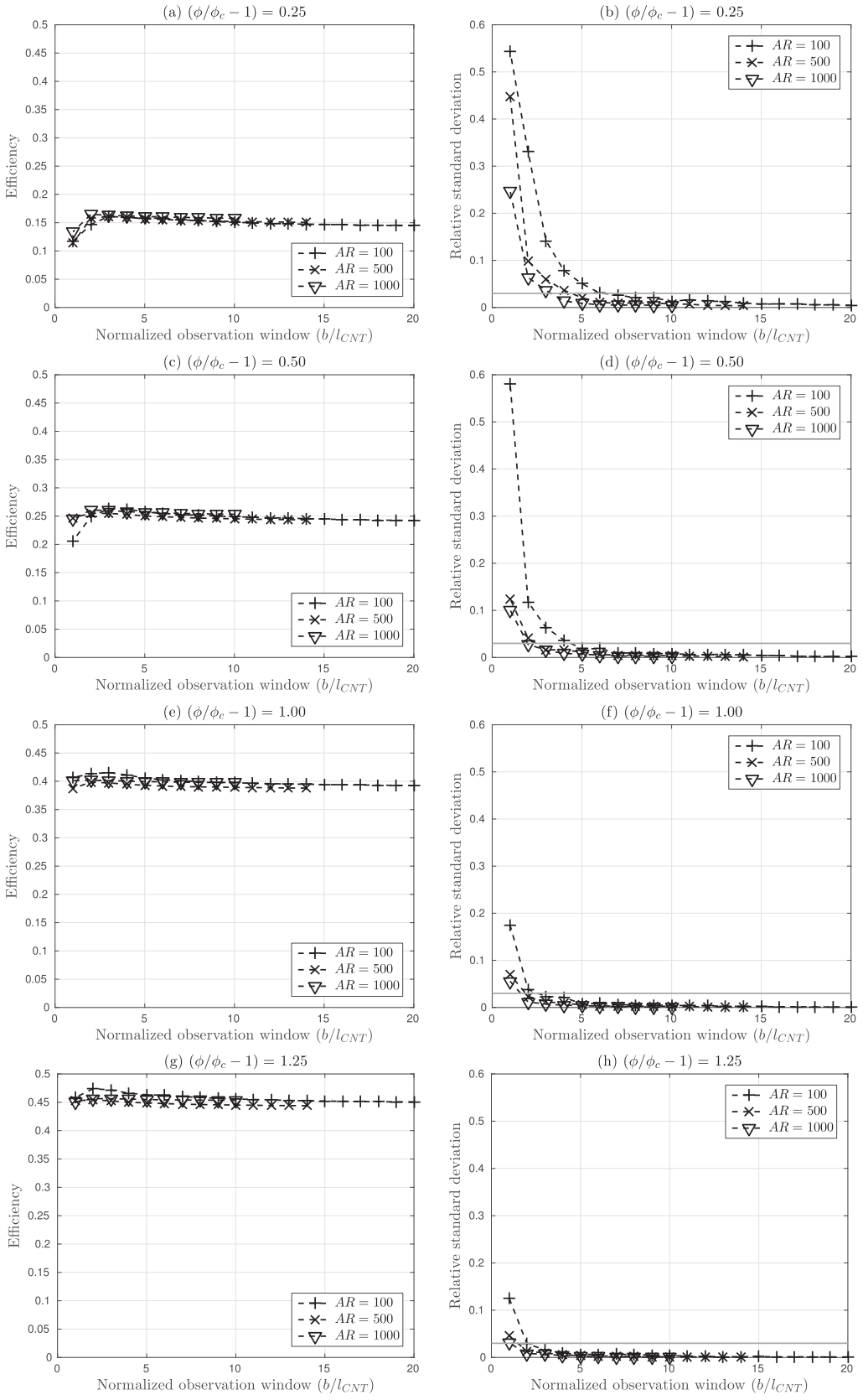

Fig. 5. Average of efficiency (left column) and its relative standard deviation (right column) over 20 samples of CNTs of different aspect ratios. The horizontal lines on the relative standard deviation plots indicate the threshold to define the size of RVE.

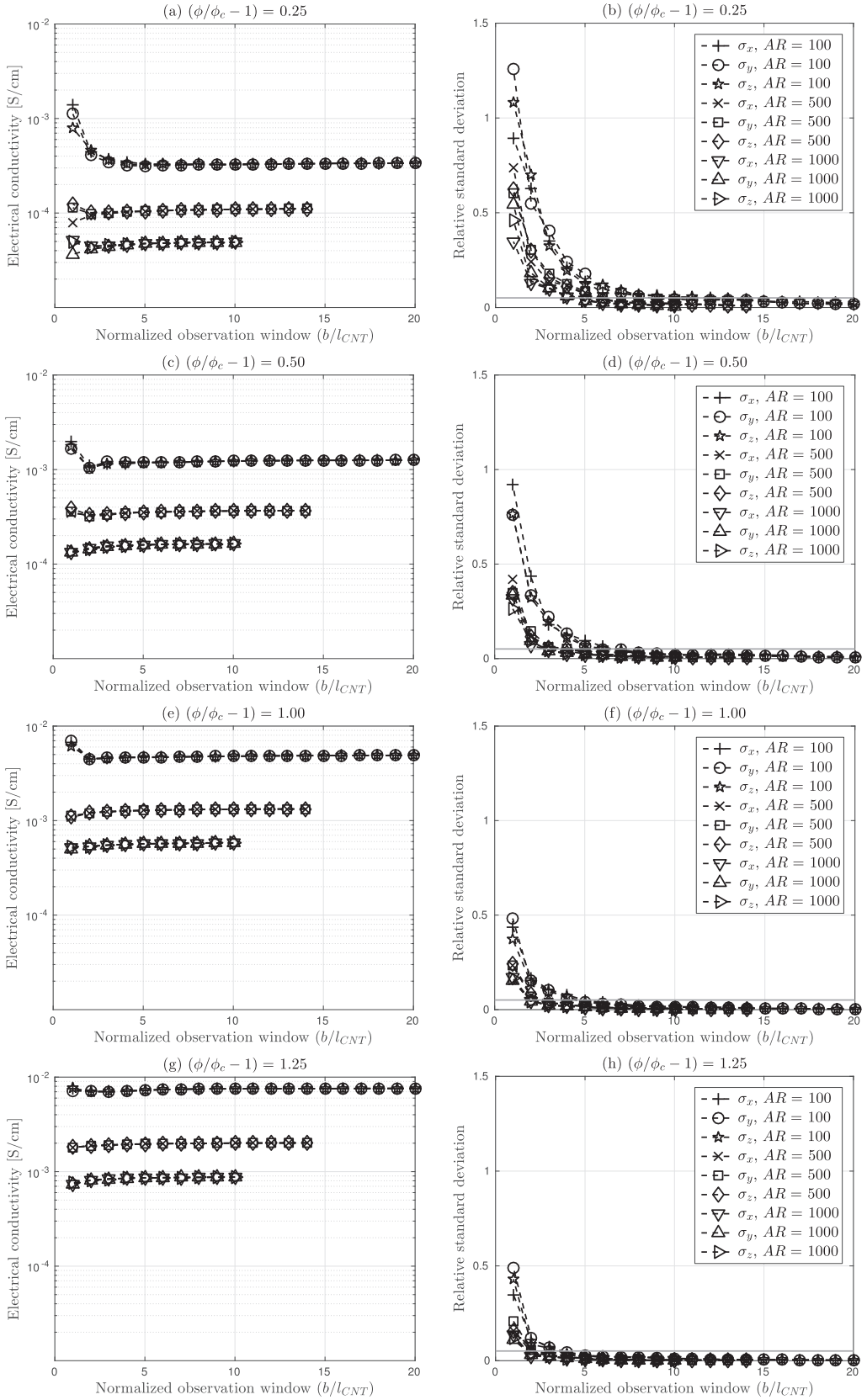

Fig. 6. Average of electrical conductivity along the three directions (left column) and relative standard deviation (right column) over 20 samples of CNTs with different aspect ratios. The horizontal lines on the relative standard deviation plots indicate the threshold to define the size of RVE.

electrical conductivity is reduced. For a given content, the electrical conductivity reaches a plateau as the observation window is increased for all aspect ratios, and it becomes isotropic before reaching this plateau.

When comparing the efficiency and the electrical conductivity (left columns of Figs. 5 and 6, respectively) at a fixed reduced volume fraction, we find that the samples with a lower aspect ratio are more conductive even though their efficiency is similar. This is due to the fact that samples with a lower aspect ratio have a larger overall volume content of CNTs. Therefore, the higher carbon content in samples of CNTs with low aspect ratios makes them more conductive. We also note that the differences in electrical conductivity remain almost the same as the reduced volume fraction is increased.

In strain sensing applications, the strain sensitivity is increased when the CNT loading is small [20,32,53]. In these cases, loadings close to the percolation threshold are more useful. We consider the higher conductivity of CNTs with low aspect ratios for similar loadings above the percolation threshold to be more suitable for strain-sensing applications. In this way, by having a higher electrical conductivity, these samples have a larger conductivity range in which a drop in conductivity can be detected. This result is in agreement with the work of Rahman and Servati [36], who found that low-aspect-ratio CNTs result in sensors with higher sensitivity.

In the right column of Fig. 6, we can see that the relative standard deviation is reduced when the size of the observation window is increased. This corresponds to a reduction in the variability of the electrical properties of the samples along the three directions. Thus, we also use a threshold equal to 5 % of the maximum relative standard deviation to determine the size of the RVE. This threshold is indicated with a horizontal line in Fig. 6(b), (d), (f), and (h).

In Fig. 7, we show the size of the RVE based on efficiency, L_{eff}, and the electrical conductivity, L_σ, as a function of the reduced volume fraction. We observe that both types of RVE can be reduced by increasing the CNT content. We also observe that $L_\sigma > L_{eff}$ for every volume fraction, indicating that the network morphology stabilizes faster than its physical properties. Thus, in order to make reliable simulations or meaningful measurements of the electrical conductivity, we should consider a sample with a size of at least L_σ.

Finally, we fit the sizes of the RVEs using a power law that depends only on the reduced volume fraction as:

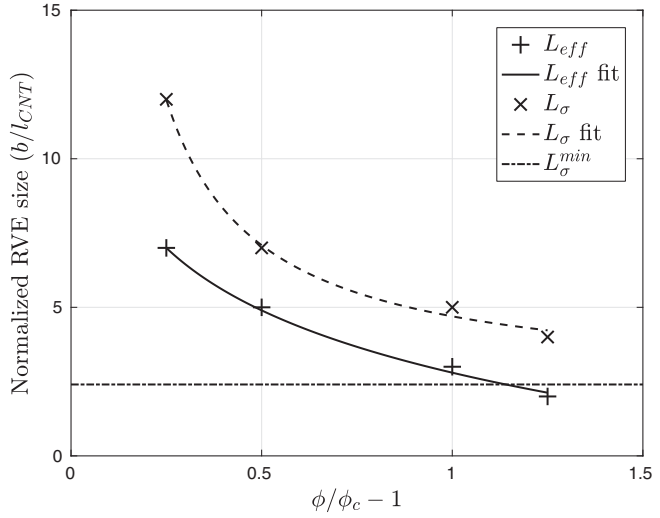

Fig. 7. RVE size as a function of reduced volume fraction for different aspect ratios. Power law fits of the form $L_X = a(\phi/\phi_c - 1)^b + c$ are also shown, where L_X stands for either L_{eff} or L_σ. The fitting parameters for L_{eff} are $a = 755.3$, $b = -0.004$, and $c = -752.5$; while for L_σ they are $a = 2.294$, $b = -1.031$, and $c = 2.403$. The horizontal line represents $L_\sigma^{min} = 2.403$, which is the minimum possible RVE size.

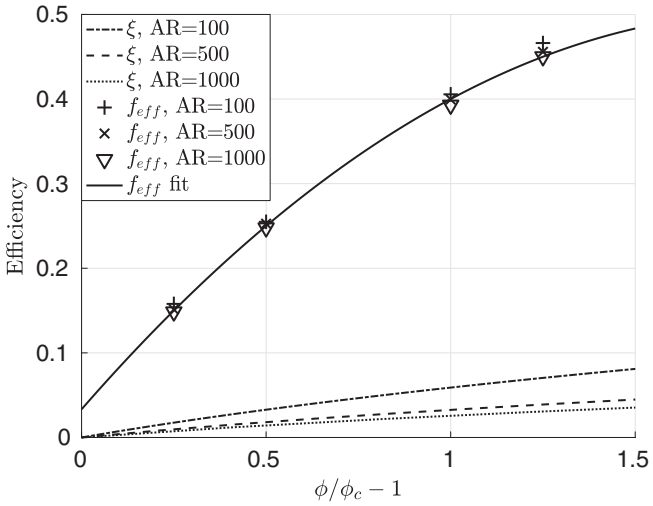

Fig. 8. Comparison of the fraction of percolated CNTs, ξ, as given by Deng and Zheng [10] with our results on efficiency, f_{eff}.

$$L_X = a(\phi/\phi_c - 1)^b + c \tag{3}$$

where L_X stands for either L_{eff} or L_σ. The fitting parameters for L_{eff} are $a = 755.3$, $b = -0.004$, and $c = -752.5$; while for L_σ they are $a = 2.294$, $b = -1.031$, and $c = 2.403$. We find that the fitting reproduces the size of the RVE very well. Thus, Eq. 3 can be used to obtain L_σ for different CNT loadings. From that equation, we note that as $\phi \to \infty$, the minimum possible RVE size, L_σ^{min}, is 2.403 times the length of the CNT. The value of L_σ^{min} is shown in Fig. 7 with an horizontal line.

3.4. Comparison of efficiency measures

We now compare our results on efficiency with results from the expression presented by Deng and Zheng [10] for percolated CNTs, ξ, which is given as:

$$\xi(\phi) = \frac{\phi^{1/3} - \phi_c^{1/3}}{1 - \phi_c^{1/3}}. \tag{4}$$

In Fig. 8, we present our results on efficiency at L_σ, shown with unconnected symbols, and compare them with those obtained with Eq. 4. The three discontinuous lines show the values of $\xi(\phi)$ for different aspect ratios. Two main differences are observed. First, our results show that efficiency is independent of the aspect ratio when plotted as a function of the reduced volume fraction. In the case of Eq. 4, as the aspect ratio becomes larger, these differences also become larger. Second, there are large differences between our results on efficiency and those obtained using Eq. 4. Given that our results are based on the analysis of actual CNT networks, we believe that Eq. 4 underestimates the amount of percolated CNTs. We found a good fit using a polynomial equation on the reduced volume fraction as:

$$f_{eff}(\phi_{red}) = p_1\phi_{red}^2 + p_2\phi_{red} + p_3, \tag{5}$$

where $\phi_{red} = \phi/\phi_c - 1$, $p_1 = -0.1333$, $p_2 = 0.5$, and $p_3 = 0.0333$. This fit is shown in Fig. 8 as a solid line.

In addition, from Eq. 4 we observe that $\xi(\phi_c) = 0$. This value does not seem realistic as it means that the percolated network has no CNTs in it. From the independent term in Eq. 5, we expect that 3.33% of CNTs will percolate at a loading equal to ϕ_c.

3.5. Network efficiency and electrical conductivity

In Fig. 9(a), we present the efficiency of CNT networks as a function of volume fraction for different aspect ratios. Again, we observe that,

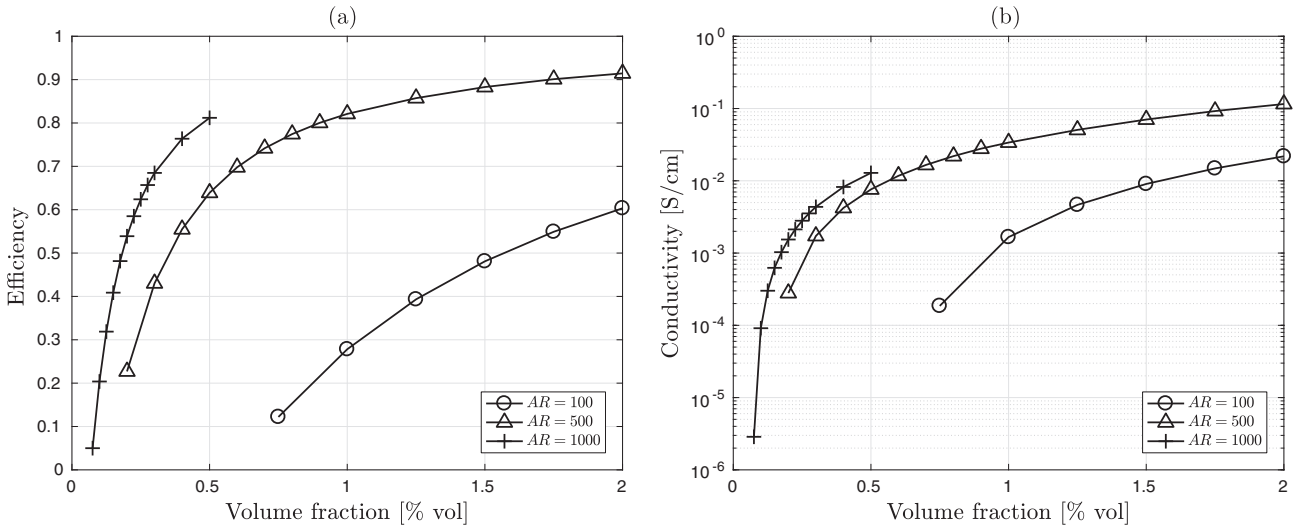

Fig. 9. Comparison of efficiency (a) and electrical conductivity (b) as a function of volume fraction for different aspect ratios.

for each aspect ratio, increasing the loading of CNTs increases the efficiency. However, the efficiency increases faster with nanotubes with a large aspect ratio. There is a large increase in the efficiency when the aspect ratio changes from 100 to 500. However, the increase is not as significant when the aspect ratio changes from 500 to 1000.

In Fig. 9(b), we present the electrical conductivity of CNT networks as a function of the volume fraction for different aspect ratios. By comparing the efficiency and conductivity plots, we observe that an increase in the efficiency correlates with an increase in conductivity. Electrical conductivity increases by increasing CNT loading, and this increase is faster with CNTs with large aspect ratios. This behavior correlates with the observations of efficiency in Fig. 9(a). We also observe that the differences in electrical conductivity are reduced by increasing volume content (when comparing the same loading). Results in Fig. 9(b) suggest that, for loadings above 0.3% volume fraction, increasing the aspect ratio above 500 does not significantly increase the electrical conductivity. Similarly, for loadings above 2% volume fraction, increasing the aspect ratio above 100 results in a small improvement in electrical conductivity. It has been reported that increasing the aspect ratio results in a lower percolation threshold and higher electrical conductivity of polymers [31,47]. However, here we show that the advantage of increasing the aspect ratio depends on the CNT loading. We also observe that the main advantage in increasing the aspect ratio above 500 is to obtain a conductive polymer with a lower CNT loading. However, these polymers are not as conductive as those with higher loadings of CNTs that have smaller aspect ratios. In addition, agglomerations and entanglement of large aspect ratio CNTs is common [5,29,31,34,50], which ultimately reduces the doping effects of the nanofiller and can result in the agglomerations acting as defect sites [45].

Given the direct relationship between efficiency and electrical conductivity, efficiency can be used as an indicator of how well the network will perform from an electrical conductivity standpoint. In addition, the use of this indicator comes at a lower computational cost compared with calculating the electrical conductivity of the network.

3.6. Sensitivity analysis of electrical parameters

The electrical conductivity of a CNT, σ_{CNT}, and the junction resistance, R_J, are two important parameters directly affecting the electrical conductivity of CNT networks. CNTs are often assumed to be perfect conductors (i.e., they have 0 Ω resistance) and are thus not included in the resistor network used to calculate the conductivity of the composite [7,11,40,48,51,56]. However, this assumption is made without proper justification. In addition, there are only a few studies investigating the effect of junction resistance on the composite's conductivity [9,24]. The actual junction resistance also depends on the electrical properties of the polymer matrix [23,31]. By studying the effects of junction resistance on the composite's conductivity, we can therefore determine how much the electrical properties of the polymer can be improved. Thus, we perform a sensitivity analysis of our model on these two parameters.

In Fig. 10(a), we show the sensitivity analysis on CNT electrical conductivity when the junction resistance is kept constant at $R_J = 10^7$ Ω. In this figure, we observe that there is no noticeable change in electrical conductivity when σ_{CNT} is above 10^2 S/cm. Thus, if the CNTs in the simulation have $\sigma_{CNT} < 10^2$ S/cm, their electrical conductivity should be included as a parameter to calculate the composite's conductivity when constructing the resistor network.

Fig. 10(b) shows the sensitivity analysis of our model on junction resistance when the conductivity of the CNT is kept constant at $\sigma_{CNT} = 10^2$ S/cm. In this figure, we observe that, for $R_J \geqslant 10^7$, a reduction of one order of magnitude in R_J results in an increase of one order of magnitude on the conductivity. This result highlights the importance of reducing the effects of the junction resistance, e.g., by coating the CNTs with a conductive polymer [16,46,54]. On the other hand, for $R_J \leqslant 10^6$ Ω, there is a small effect of the junction resistance on the conductivity of the composite. If the junction resistance is already on the order of 10^6 Ω, there is no advantage to trying to reduce its value further.

4. Conclusions

We developed a computational tool that generates geometrical representations of CNT networks. We provided a definition of efficiency based on the backbone of these CNT networks. This definition of efficiency is meaningful for evaluating, at minimal computational cost, how well the network will perform from an electrical conductivity standpoint. In this study, we introduced an expression that can be used to obtain the size of the RVE for any CNT loading. This expression tells us that the RVE size cannot be smaller than 2.4 times the length of the CNT and that it will increase by reducing volume content. We proposed a simplified formula to estimate the efficiency that shows that at least 3.33% of CNTs contribute to electrical conductivity at a loading equal to the percolation threshold.

By studying the efficiency and conductivity of polymers loaded with CNTs, we found that increasing the aspect ratio of CNTs generally results in more efficient and conductive polymers. We also found that the

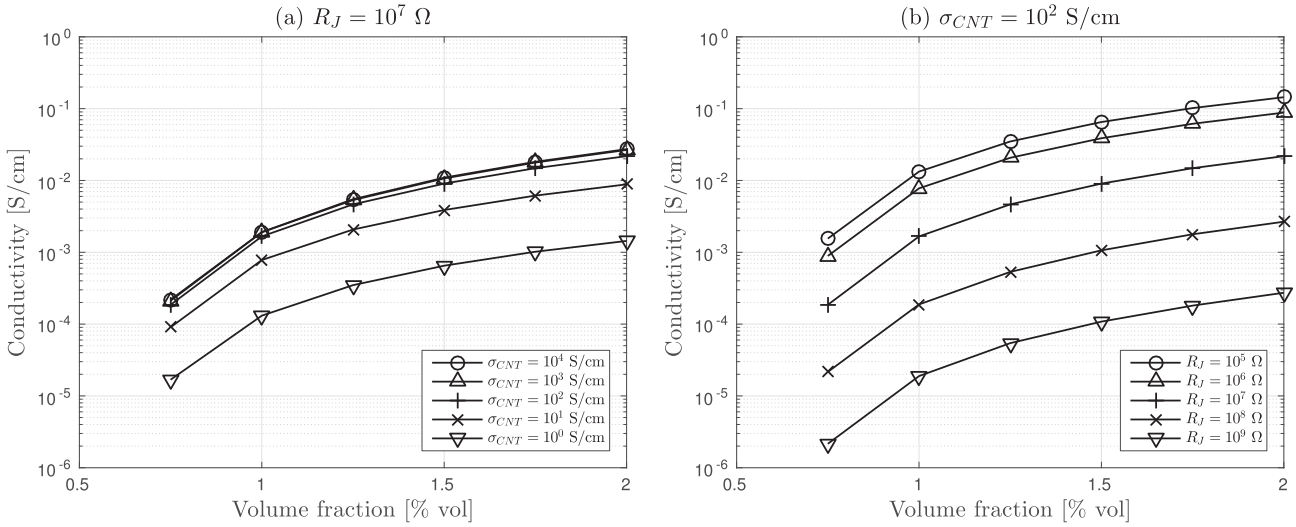

Fig. 10. Sensitivity analysis of (a) CNT electrical conductivity, and (b) junction resistance.

benefit of increasing the aspect ratio depends on the CNT content. Aspect ratios of 1000 result in more conductive polymers at loadings below 0.3% volume fraction, while aspect ratios of 500 are more suitable for loadings between 0.3% and 2% volume fraction.

Finally, we performed a sensitivity analysis on the electrical conductivity of CNTs and junction resistance. We found that CNTs with conductivities below 10^2 S/cm should not be ignored when calculating the composite's conductivity. This is contrary to the common practice of ignoring the conductivity of the nanofiller. We found that a reduction in the junction resistance by one order of magnitude could lead to an increase in the composite's conductivity by one order of magnitude. This highlights the importance of reducing the junction resistance. However, if the value of the junction resistance is already around 10^6 Ω, there is no benefit in further reducing it.

Data availability statement

The raw/processed data required to reproduce these findings cannot be shared at this time as the data also forms part of an ongoing study.

Acknowledgement

The research reported in this publication was funded by King Abdullah University of Science and Technology (KAUST).

References

[1] Aguilar Ventura I, Zhou J, Lubineau G, Lubineau G. Drastic modification of the piezoresistive behavior of polymer nanocomposites by using conductive polymer coatings. Compos Sci Technol 2015;117:342–50.
[2] Babalievski F. Cluster counting: the Hoshen-Kopelman algorithm vs. spanning tree approaches. Int J Mod Phys C 1998;9(1):18.
[3] Bauhofer W, Kovacs JZ. A review and analysis of electrical percolation in carbon nanotube polymer composites. Compos Sci Technol 2009;69(10):1486–98.
[4] Benoit JM, Corraze B, Lefrant S, Bernier P, Chauvet O. Electric transport properties and percolation in carbon nanotubes/PMMA composites. MRS Proc 2001;706.
[5] Brigandi PJ, Cogen JM, Reffner JR, Wolf CA, Pearson RA. Influence of carbon black and carbon nanotubes on the conductivity, morphology, and rheology of conductive ternary polymer blends. Polym Eng Sci Eng 2017;57(12):1329–39.
[6] Buldum A, Lu JP. Contact resistance between carbon nanotubes. Phys Rev B 2001;63(16). 161403–1–4.
[7] Castellino M, Rovere M, Shahzad MI, Tagliaferro A. Conductivity in carbon nanotube polymer composites: a comparison between model and experiment. Compos Part A: Appl Sci Manuf 2016;87:237–42.
[8] Chang L, Friedrich K, Ye L, Toro P. Evaluation and visualization of the percolating networks in multi-wall carbon nanotube/epoxy composites. J Mater Sci 2009;44(15):4003–12.
[9] De Vivo B, Lamberti P, Spinelli G, Tucci V. Numerical investigation on the influence factors of the electrical properties of carbon nanotubes-filled composites. J Appl Phys 2013;113(24):244301.
[10] Deng F, Zheng Q-S. An analytical model of effective electrical conductivity of carbon nanotube composites. Appl Phys Lett 2008;92(7):071902.
[11] Eken AE, Tozzi EJ, Klingenberg DJ, Bauhofer W. A simulation study on the combined effects of nanotube shape and shear flow on the electrical percolation thresholds of carbon nanotube/polymer composites. J Appl Phys 2011;109(8):084342.
[12] Feng C, Jiang L. Micromechanics modeling of the electrical conductivity of carbon nanotube (CNT)-polymer nanocomposites. Compos Part A: Appl Sci Manuf 2013;47:143–9.
[13] Fuhrer MS. Crossed nanotube junctions. Science 2000;288(5465):494–7.
[14] García-Macías E, D'Alessandro A, Castro-Triguero R, Pérez-Mira D, Ubertini F. Micromechanics modeling of the uniaxial strain-sensing property of carbon nanotube cement-matrix composites for SHM applications. Compos Struct 2017;163:195–215.
[15] Han F, Azdoud Y, Lubineau G. Computational modeling of elastic properties of carbon nanotube/polymer composites with interphase regions. Part I: microstructural characterization and geometric modeling. Comput Mater Sci 2014;81:641–51.
[16] Hermant MC, Klumperman B, Kyrylyuk AV, van der Schoot P, Koning CE. Lowering the percolation threshold of single-walled carbon nanotubes using polystyrene/poly(3,4-ethylenedioxythiophene): poly(styrene sulfonate) blends. Soft Matter 2009;5(4):878.
[17] Hoshen J, Kopelman R. Percolation and cluster distribution I Cluster multiple labeling technique and critical concentration algorithm. Phys Rev B 1976;14(8):3438–45.
[18] Hu N, Karube Y, Yan C, Masuda Z, Fukunaga H. Tunneling effect in a polymer/carbon nanotube nanocomposite strain sensor. Acta Mater 2008;56(13):2929–36.
[19] Kennel EB. Electrical properties of nanoparticle-filled polymers. Polymer nanocomposites handbook, chapter 16. CRC Press; 2009.
[20] Ku-Herrera JJ, Avilés F, Seidel GD. Self-sensing of elastic strain, matrix yielding and plasticity in multiwall carbon nanotube/vinyl ester composites. Smart Mater Struct 2013;22(8):085003.
[21] Li C, Chou T-W. A direct electrifying algorithm for backbone identification. J Phys A: Math Theor 2007;40(49):14679–86.
[22] Li C, Chou T-W. Precise determination of backbone structure and conductivity of 3D percolation networks by the direct electrifying algorithm. Int. J Mod Phys C 2009;20(800):422–33.
[23] Li C, Chou T-W. Electrical conductivities of composites with aligned carbon nanotubes. J Nanosci Nanotechnol 2009;9(4):2518–24.
[24] Li C, Thostenson ET, Chou T-W. Dominant role of tunneling resistance in the electrical conductivity of carbon nanotube-based composites. Appl Phys Lett 2007;91(22):223114.
[25] Li C, Thostenson ET, Chou T-W. Effect of nanotube waviness on the electrical conductivity of carbon nanotube-based composites. Compos Sci Technol 2008;68(6):1445–52.
[26] Li C, Thostenson ET, Chou T-W. Sensors and actuators based on carbon nanotubes and their composites: a review. Compos Sci Technol 2008;68(6):1227–49.
[27] Lubineau G, Mora A, Han F, Odeh IN, Yaldiz R. A morphological investigation of conductive networks in polymers loaded with carbon nanotubes. Comput Mater Sci 2017;130:21–38.
[28] Ma X, Scarpa F, Peng HX, Allegri G, Yuan J, Ciobanu R. Design of a hybrid carbon fibre/carbon nanotube composite for enhanced lightning strike resistance. Aerosp Sci Technol 2015;47:367–77.
[29] Mierczynska A, Mayne-L'Hermite M, Boiteux G, Jeszka JK. Electrical and mechanical properties of carbon nanotube/ ultrahigh-molecular-weight polyethylene composites prepared by a filler prelocalization method. J Appl Polym Sci 2007;105:158–68.

[30] Mora A, Han F, Lubineau G. Computational modeling of electrically conductive networks formed by graphene nanoplatelet–carbon nanotube hybrid particles. Modell Simul Mater Sci Eng 2018;26(3):035010.
[31] Mutiso RM, Winey KI. Electrical properties of polymer nanocomposites containing rod-like nanofillers. Prog Polym Sci 2015;40:63–84.
[32] Nanni F, Mayoral BL, Madau F, Montesperelli G, McNally T. Effect of MWCNT alignment on mechanical and self-monitoring properties of extruded PET-MWCNT nanocomposites. Compos Sci Technol 2012;72(10):1140–6.
[33] Oliva-Avilés AI, Avilés F, Seidel GD, Sosa V. On the contribution of carbon nanotube deformation to piezoresistivity of carbon nanotube/polymer composites. Compos Part B: Eng 2013;47:200–6.
[34] Pan Y, Li L, Chan SH, Zhao J. Correlation between dispersion state and electrical conductivity of MWCNTs/PP composites prepared by melt blending. Compos Part A: Appl Sci Manuf 2010;41(3):419–26.
[35] Pang H, Xu L, Yan DX, Li ZM. Conductive polymer composites with segregated structures. Prog Polym Sci 2014;39(11):1908–33.
[36] Rahman R, Servati P. Effects of inter-tube distance and alignment on tunnelling resistance and strain sensitivity of nanotube/polymer composite films. Nanotechnology 2012;23(5):055703.
[37] Ramasubramaniam R, Chen J, Liu H. Homogeneous carbon nanotube/polymer composites for electrical applications. Appl Phys Lett 2003;83(14):2928–30.
[38] Seidel GD, Lagoudas DC. A micromechanics model for the electrical conductivity of nanotube-polymer nanocomposites. J Compos Mater 2009;43(9):917–41.
[39] Seidel GD, Puydupin-Jamin AS. Analysis of clustering, interphase region, and orientation effects on the electrical conductivity of carbon nanotube-polymer nanocomposites via computational micromechanics. Mech Mater 2011;43(12):755–74.
[40] Simoneau L-P, Villeneuve J, Aguirre CM, Martel R, Desjardins P, Rochefort A. Influence of statistical distributions on the electrical properties of disordered and aligned carbon nanotube networks. J Appl Phys 2013;114(11):114312.
[41] Smith JG, Connell JW, Delozier DM, Lillehei PT, Watson KA, Lin Y, et al. Space durable polymer/carbon nanotube films for electrostatic charge mitigation. Polymer 2004;45(3):825–36.
[42] Song W, Krishnaswamy V, Pucha RV. Computational homogenization in RVE models with material periodic conditions for CNT polymer composites. Compos Struct 2016;137:9–17.
[43] Stauffer D, Aharony A. 2nd ed. Introduction to percolation theory Taylor & Francis; 1994.
[44] Sun X, Song M. Highly conductive carbon nanotube/polymer nanocomposites achievable? Macromol Theory Simul 2009;18(3):155–61.
[45] Truong VT, Tsang KMC, Keough SJ, St John NA. Effect of sonication on the mechanical properties of poly (vinyl alcohol)/carbon nanotube composites. Smart Mater, Nano- Micro-Smart Syst 2007;6415:641503.
[46] Ventura IA, Zhou J, Lubineau G. Investigating the inter-tube conduction mechanism in polycarbonate nanocomposites prepared with conductive polymer-coated carbon nanotubes. Nanoscale Res Lett 2015;10(1):485.
[47] Wernik JM, Meguid SA. Recent developments in multifunctional nanocomposites using carbon nanotubes. Appl Mech Rev 2010;63(5):050801.
[48] White SI, DiDonna BA, Mu M, Lubensky TC, Winey KI. Simulations and electrical conductivity of percolated networks of finite rods with various degrees of axial alignment. Phys Rev B – Condens Matter Mater Phys 2009;79(2). 024301-1-6.
[49] Winey KI, Kashiwagi T, Mu M. Improving electrical conductivity and thermal properties of polymers by the addition of carbon nanotubes as fillers. MRS Bull 2007;32:348–53.
[50] Xin F, Li L. Decoration of carbon nanotubes with silver nanoparticles for advanced CNT/polymer nanocomposites. Compos Part A: Appl Sci Manuf 2011;42(8):961–7.
[51] Yu Y, Song G, Sun L. Determinant role of tunneling resistance in electrical conductivity of polymer composites reinforced by well dispersed carbon nanotubes. J Appl Phys 2010;108(8):084319.
[52] Zare Y, Rhee KY. A simple model for electrical conductivity of polymer carbon nanotubes nanocomposites assuming the filler properties, interphase dimension, network level, interfacial tension and tunneling distance. Compos Sci Technol 2018;155:252–60.
[53] Zetina-Hernández O, Duarte-Aranda S, May-Pat A, Canché-Escamilla G, Uribe-Calderon J, Gonzalez-Chi PI, Avilés F. Coupled electro-mechanical properties of multiwall carbon nanotube/polypropylene composites for strain sensing applications. J Mater Sci 2013;48(21):7587–93.
[54] Zhou J, Lubineau G. Improving electrical conductivity in polycarbonate nanocomposites using highly conductive PEDOT/PSS coated MWCNTs. ACS Appl Mater Interfaces 2013;5(13). 6189-200.
[55] Zhou J, Yu H, Xu X, Han F, Lubineau G. Ultrasensitive, stretchable strain sensors based on fragmented carbon nanotube papers. ACS Appl Mater Interfaces 2017;9(5):4835–42.
[56] Zurita-Gotor M, Gittleson FS, Taylor AD, Blawzdziewicz J. Stratified rod network model of electrical conductance in ultrathin polymer–carbon nanotube multilayers. Phys Rev B 2013;87(19):195449.